Rotational dynamics of proteins from spin relaxation rates and molecular dynamics simulations

O. H. Samuli Ollila*
Insititute of Biotechnology, University of Helsinki
(Dated: June 16, 2017)

I. INTRODUCTION

Protein conformational sampling and entropy plays significant role in protein functionality and interactions with other biomolecules. The related Protein backbone and side chains dynamics as well as protein overall brownian tumbling can be experimentally studied by using NMR relaxation experiments of backbone N-H or side chain ?? bonds [1–3]. Spin relaxation data is usually analyzed by describing the sampled bond orientations with order parameter S^2 respect to the protein reference frame and assuming that overall and internal motions are independt [2**?**]. Order parameters and timescales for overall and internal motions can be then extracted by fitting various functional forms to spin relaxation data measured with different magnetic field strengths [1, 2].

This approach has been successfully applied for large amount of proteins with isotropic shape and overall rotational diffusion [1]. The resulting order parameters and overall rotational diffusion coefficients have been used in wide range applications, including analysis of conformational entropy [**?**], binding entropy of ?? [**?**], resolving sampled structures [**?**] and validating molecular dynamics simulations [**?**].

Two different approaches have been commonly used to analyze rotational dynamics from NMR relaxation experiments. In "model free analysis" the fundamental idea is to separate interal dynamics from global rotation and assume exponential forms for rotational correlation functions. The parameters of rotational correlation functions are then fitted the experimental data to solve time scales and order parameters for different dynamical processes [**?**]. Alternative approach is to use bead models and hydrodynamical calculations to describe protein dynamics and predict spin relaxation rates [**?**]. The approaches have been successfull or several proteins, but both suffer from significant limitations which limit the general applicability [**?**]. Main practical issue in the "model free analysis" is that the amount of freen parameters to be fitted in the experiments becomes large for anitoropic proteins experiencing complex dynamics [**?**]. On the other hand, hydrodynamical calculations are sentitive for the assumptions about protein hydration shell [**?**].

Classical molecular dynamics simulations have been considered as a promising tool for interpretation of rotational motions from NMR relaxation data, because they simultaneously contain internal rotation, global browian tumbling, anisotropy and hydration shell effects [**?**]. However, practical applications have been limited by the inaccuracies in force field descriptions and available time scales in the simulations. The most used water model in rotational dynamics studies, tip3p [**?**], predicts too fast rotational diffusion [**?**]. On the other hand, very long simulations are needed to collect enough statistics to calculate rotational correlation functions from single molecules in MD simulations [**?**]. Consequnetly, protein rotational diffusion coefficients are not typically calculated from simulation data. Instead, the calculated relaxation rates are fitted to experiments by assuming an isotropic diffusion model [**?**].

In this work we overcome these issues by directly calculating diffusion coefficients from protein intertia axes. Diffusion coefficients can be then used to determine global rotational correlation functions from shorter simulations than with direct calculation. Furthermore, the oversestimated dynamics due to water model can be anisotropically corrected by scaling the diffusion coefficients with a constant factor. The usefullness of the approach is demonstrated by interpreting the spi relaxation data from aniotropic protein constructs from TonB of Helicobacteri pyroli [**?**] and Pseudomonas [**?**]. These segments are considered as vital parts related to iron transport into Gran-negative bacteria [**?**].

II. METHODS

A. Spin relaxation and rotational dynamics of molecules

Practical approaches to analyze molecular dynamics from NMR relaxation data are usually based on the connection between second order rotational correlation function $C(t)$ of N-H bond and experimentally measured spin relaxation rates R_1, R_2 and R_{NOE} through Redfield equations [4, 5]

$$R_1 = \frac{d_{\mathrm{NH}}^2 N_{\mathrm{H}}}{20}\left[J(\omega_{\mathrm{H}}-\omega_{\mathrm{N}}) + 3J(\omega_{\mathrm{N}}) + 6J(\omega_{\mathrm{N}}+\omega_{\mathrm{H}})\right] + \frac{(\sigma\omega_{\mathrm{N}})^2}{15} j(\omega_{\mathrm{N}}), \tag{1}$$

$$R_2 = \frac{1}{2}\frac{d_{\mathrm{NH}}^2 N_{\mathrm{H}}}{20}\left[4J(0) + 3j(\omega_{\mathrm{N}}) + J(\omega_{\mathrm{H}}-\omega_{\mathrm{N}}) + 6J(\omega_{\mathrm{H}}) + 6J(\omega_{\mathrm{N}}+\omega_{\mathrm{H}})\right] + \frac{(\sigma\omega_{\mathrm{N}})^2}{15*6}[4J(0)+3J(\omega_{\mathrm{N}})], \tag{2}$$

$$R_{\mathrm{NOE}} = 1 + \frac{d_{\mathrm{NH}}^2 N_{\mathrm{H}}}{20}\left[6J(\omega_{\mathrm{N}}+\omega_{\mathrm{H}}) + J(\omega_{\mathrm{H}}-\omega_{\mathrm{N}}))\right]\frac{\gamma_{\mathrm{H}}}{\gamma_{\mathrm{N}} R_1}, \tag{3}$$

where ω_{N} and ω_{H} are the Larmor angular frequencies of ^{15}N and ^{1}H respectively, and N_{H} is the number of bound protons.

* samuli.ollila@helsinki.fi; Department of Neuroscience and Biomedical Engineering, Aalto University

Spectral density $J(\omega)$ is the Fourier transformation of the second order rotational correlation function for N-H bond

$$J(\omega) = 2\int_0^\infty C(t)\cos(\omega t)\mathrm{d}t. \quad (4)$$

The second order rotational correlation is defined as

$$C(t) = \langle(3\cos^2\theta_{t';t'+t} - 1)/2\rangle_{t'}, \quad (5)$$

where average is ensemble average and θ is the angle between N-H bonds at times t' and $t'+t$. The dipolar coupling constant is given by

$$d_{\mathrm{NH}} = -\frac{\mu_0\hbar\gamma_{\mathrm{H}}\gamma_{\mathrm{N}}}{4\pi\langle r^3_{\mathrm{CN}}\rangle},$$

where μ_0 is the magnetic constant or vacuum permeability, $\hbar$ is the reduced Planck constant, γ_{N} and γ_{H} are the gyromagnetic constants of ^{15}N and ^{1}H, respectively. Average cubic length is $\langle r^3_{\mathrm{CN}}\rangle \approx$ and the chemical shift anisotropy is $\Delta\sigma \approx 160 * 10^{-6}$ for N-H bonds in proteins [**?**]. Same equations can be used, for example, to C-H bond by changing the constants related to nitrogen to the ones corresponding carbon.

Experimental spin relaxation rates of proteins are typically intepreted by assuming that the global and interal rotational dynamics are independent. The rotational correlation function for each bond can be then written as [**?**]

$$C(t) = C_I(t)C_O(t), \quad (6)$$

where $C_I(t)$ and $C_O(t)$ are correlation functions for internal and overall rotiations, respectively. Within this approximation the internal rotational correlation function decays to a plateau, which defines the square of order parameter respect to molecular axes S^2. Timescale for internal relaxation dynamics can be estimated by using the effective internal correlation time

$$\tau_{\mathrm{eff}} = \int_0^\infty C'_I(t)\mathrm{d}t, \quad (7)$$

where $C'_I(t) = (C_I - S^2)/(1 - S^2)$ is the reduced correlation function [**?**].

The global rotational dynamics for fully anisotropic molecule can be described as a sum of five exponentials [**?**]

$$C_O(t) = \sum_{j=1}^{5} A_j e^{-t/\tau_j}, \quad (8)$$

where time constants τ_j are related [6] to the diffusion constants around three principal axes of a molecule (D_{xx}, D_{yy} and D_{zz}) and prefactors A_j can be related to the directions of bond respect to the principal axes. The rotational diffusion constants are defined as

$$\begin{aligned}\langle(\Delta\alpha_{t';t'+t})^2\rangle_{t'} &= 2D_{xx}t\\ \langle(\Delta\beta_{t';t'+t})^2\rangle_{t'} &= 2D_{yy}t\\ \langle(\Delta\gamma_{t';t'+t})^2\rangle_{t'} &= 2D_{zz}t,\end{aligned} \quad (9)$$

where $\langle(\Delta\alpha_{t';t'+t})^2\rangle_{t'}$, $\langle(\Delta\beta_{t';t'+t})^2\rangle_{t'}$ and $\langle(\Delta\gamma_{t';t'+t})^2\rangle_{t'}$ are mean square angle deviations of protein intertia axes.

The internal and overall correlation functions are monoexponential for proteins with isotropic overall rotational diffusion and single timescale for internal motion. The dynamics of such proteins is described with three parameters in the original "model free analysis"; internal rotational relaxation time τ_e, global rotaional relaxation time τ_c and the order parameter S^2. The values for these parameters can be then determined by fitting the Eqs. 1-8 to experimental spin relaxation data [**?**]. However, the amount of exponentials needed to describe correlation functions, and thus the free parameters, in such fit increases if proteins experience anisotropic overall diffusion or several internal timescales. Thus the "model free analysis" becomes less applicable for proteins with significant anisotropy or more complicated internal dynamics.

B. Rotational dynamics from molecular dynamics simulations

Classical molecular dynamics simulation gives a trajectory for each atom in a system as a function of time. These trajectories can be used to calculate rotational correlation functions for each bond from Eq. 5. The rotational correlation functions can be further used to calculate the spin relaxation times through Eqs. 1-4 and the resulting values can be compared to experimental data in order to assess simulation model quality [**?**] and interpret experiments [**?**]. However, the comparison is often complicated by the short simulation times [**?**] and incorrect overall rotational diffusion due to water models [**?**].

Here we use overall rotational diffusion constants calculated from Eq. 9 to determine the timescales of global rotational correlation function in Eq. 8. The rotational diffusion coefficients are given by a linear fit to the mean square angle deviation of intertia axes calculated from simulations (see results and discussion). Straight line has only one parameter (slope) to be fitted, in contrast to multiexponential sum in Eq. 8 with ten parameters. Thus, the calculation of timescales through overall rotational diffusion constants is numerically more robust and requires less simulation data than a direct fit of Eq. 8 to the rotational correlation function calculated from simulation. The prefactors in 8 are determined by fitting to correlation function calculated from simulations, but timescales from rotational diffusion coefficients are used. The rotational diffusion constants can be also scaled with a constant factor and new correlation functions calculated to compensate the incorrect rotational diffusion due to water model in spin relaxation rate calculations.

The analysis can be divided in essentially six steps:
1) Total rotational correlation functions $C(t)$ for protein N-H bonds are calculated from MD simulation trajectory by applying Eq. 5.

2) Rotational correlation functions for internal dynamics $C_I(t)$ are calculated from a trajectory from where the overall rotation of protein is removed.
3) The overall and internal motions are assumed to be independent and overall rotational correlation function is calculated as $C_O(t) = C(t)/C_I(t)$ according to Eq. 6.
4) The protein axes of inertia and their mean square deviations as function of time are calculated from MD simulation trajectory.
5) Rotational diffusion constants D_x, D_y and D_z are calculated by fitting a straight line to mean square angle deviations of inertia axes according to Eq. 9.
6) Timescales in Eq. 8 are calculated from diffusion constants and weighting factors A_j are determined by fitting the equation to rotational correlation functions of overall rotational motion $C_0(t)$ determined in step 3.
7) New total rotational correlation functions based on Eqs. 6 and 8 are determined as

$$C_N(t) = C_I(t) \sum_{j=1}^{5} A_j e^{-t/\tau_j}, \tag{10}$$

where internal correlation function $C_I(t)$ is taken from step 2, τ_i values from rotational diffusion constants (step 5) and prefactors A_j from step 6. The incorrect rotational diffusion due to water model can be compensated in new correlation functions at this point by scaling the rotational diffusion coefficients with a constant factor.

C. Simulation and analysis details

Simulations were ran using Gromacs 5 [7] And Amber ff99SB- ILDN [8] force field for proteins . The proteins were solvated to tip3p[9], tip4p [9] or OPC4 [10] water models. NMR structures from [**?**] and [11] are used as initial structure for PaTonB and HpTonB-92, respectively. Temperature was coupled to desired value with v-rescale thermistat [12] and pressure was isotropically set to 1 bar using Parrinello-Rahman barostat [13]. Timestep was 2 fs, Lennart-Jones interactions were cut-off at 1.0 nm, PME [14, 15] was used for electrostatics and LINCS was used to constraint all bond lengths [16]. Simulation trajectory and related files are available at [??]. The simulated systems are listed in Table I

Rotational correlation functions are calculated with *gmx rotacf* and overall rotation for $C_I(t)$ calculation is removed by using fit option in *gmx trjconv* grom Gromacs package [17]. Inertia axes of protein for rotational diffusion calculation are calculated with *compute_inertia_tensor* from MDTraj python library [18]. For spectral density calculation a sum of 471 exponentials having correlation times from 1 ps to 50 ns with logarithmic spacing

$$C_N(t) = \sum_{i=1}^{N} \alpha_i e^{-t/\tau_i} \tag{11}$$

were fitted to the new correlation function calculated from Eq. 10 by using the *lsqnonneg* routine in MATLAB [19]. The Fourier transform is then calculated by using analytical function for the sum of exponentials

$$J(\omega) = 4 \sum_{i=1}^{N} \alpha_i \frac{\tau_i}{1 + \omega^2 \tau_i^2}. \tag{12}$$

Similar approach is used previously for lamellar systems in combination with solid state NMR experiements [20, 21].

III. RESULTS AND DISCUSSION

A. Global rotational dynamics of protein

The mean square angle deviations as a function of time for protein inertia axes are shown in Fig. 1 for PsTonB simulation with OPC4 water model, which the longest data set in this work (1.2μs). Linear behaviour of root mean square angle deviations are observed for the lag times up to 12 ns, suggesting that the protein follows linear diffusion model with a good approximation. Plot with log-log scale in Fig. 9 B) reveals a weakly subdiffusive region only below very short timescales of approximately 0.12 ns. Deviations from linear behaviour are also seen with longer lag times than the one hundreth of the simulation lenght as demontrated for shorter simulations in Figs. **??**. This is expected to be the maximum lag time for a good statistics for rotational dynamics analyzed from a single molecule in MD simulations [**?**]. Thus, we conclude that the rotational diffusion coefficients of protein can be calculated from the slope of mean square angle deviations according to Eq. 9 by using lag times less than one hundreth of the total MD simulation length.

The resulting rotational diffusion constants from different simulations are shown in Table I. The values are in line with previously reported experimental and simulation for different proteins with similar size [22**?**]. As expected, rotational diffusion increase with the temperature and decrease with the size of a protein. Exceptionally large diffusion constants from simulations with tip3p water model are also previously observed and explained with overestimated water self diffusion [22].

Separation of N-H bond rotational correlation functions to internal and overall contributions is exemplified in Fig. 2 for flexible loop (residue 322), β-sheet (residue 331) and flexible C-terminus (residue 341) of PsTonB. The total correlation functions calculated from original MD trajectories in Fig. 2 A) (solid lines) decay toward zero within $\sim$10-50 ns. Statistical fluctuations become visible with lag times close to one hundredth of total simulation time (approximately 4-12ns for the studied systems), which is expected to be the limit for good statistic from single molecule MD simulation [**?**]. Internal correlation functions calculated from trajectory with removed overall protein rotation in Fig. 2 B) show a decay to a plateau value, which defines the square of the order parameter S^2. The N-H bond in α-helix has largest order parameter value and fastest decay to it. Significantly lower order parameters and

TABLE I. Simulated systems and rotational diffusion coefficients (rad$^2 \cdot 10^7$/s) calculated from simulations.

Protein	Water model	T (K)	$t_{\rm sim}$ (ns)	$t_{\rm anal}$ (ns)	D_{xx}	D_{yy}	D_{zz}	$D_{||}/D_{+}$	D_{av}	files
PaTonB	tip4p	298	400	390	1.81 ± 0.01	2.06 ± 0.03	4.55 ± 0.03	2.35 ± 0.04	2.80 ± 0.02	[**?**]
PaTonB	tip4p	310	400	390	2.60 ± 0.02	2.22 ± 0.05	5.0 ± 0.1	2.07 ± 0.09	3.26 ± 0.07	[**?**]
PaTonB	OPC4	310	1200	1190	2.01 ± 0.01	2.19 ± 0.01	5.01 ± 0.03	2.39 ± 0.02	3.07 ± 0.01	[**?**]
HpTonB-92	tip3p	310	570	370	8.25 ± 0.05	7.67 ± 0.06	15.9 ± 0.3	1.99 ± 0.06	10.6 ± 0.2	[**?**]
HpTonB-92	tip3p	303	800	790	6.24 ± 0.02	7.04 ± 0.03	11.9 ± 0.2	1.80 ± 0.03	8.40 ± 0.07	[**?**]
HpTonB-92	tip4p	310	470	370	3.6 ± 0.1	3.24 ± 0.01	6.3 ± 0.3	1.8 ± 0.1	4.4 ± 0.2	[**?**]
HpTonB-92	tip4p	303	400	200	2.7 ± 0.1	2.71 ± 0.02	5.6 ± 0.5	2.1 ± 0.2	3.7 ± 0.2	[**?**]
HpTonB-92	OPC4	310	800	790	2.85 ± 0.01	2.70 ± 0.01	5.56 ± 0.01	2.00 ± 0.01	3.70 ± 0.01	[**?**]

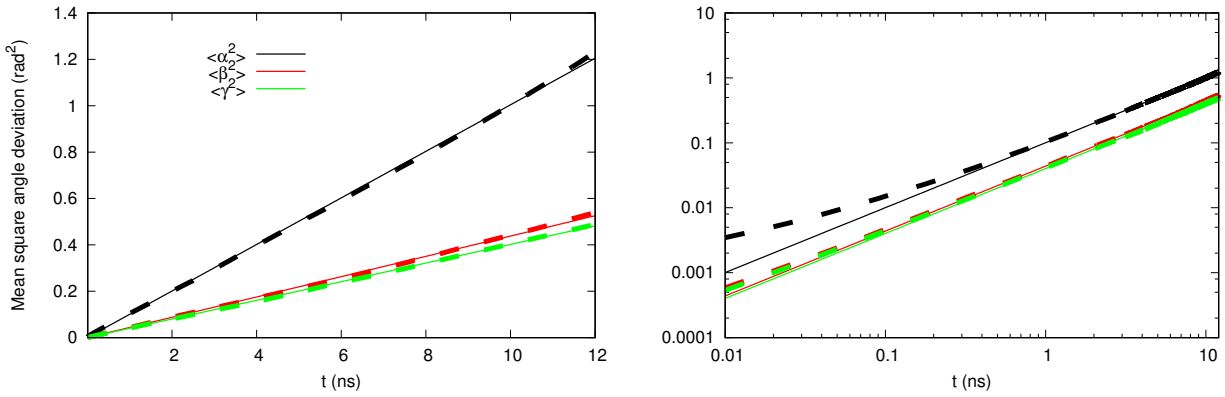

FIG. 1. The intertia tensor angles as a function of time and mean square angular deviations for PsTonB simulation with OPC water model.

slower decay are observed for bonds in loop and C-terminus can be exlpained by a larger ensemble of sampled conformations for these regions. The global rotational correlation functions shown similar slow decay from the overall rotational diffusion for all the analyzed bonds in different protein regions in Fig. 2 C) (solid lines). Global rotational correlation function for flexible C-terminus (residue 341) shows large statistical fluctuations due to small contribution from overall rotation dynamics to the total correlation function for segments with small order parameters rapid internal fluctuations.

The overall rotational correlation functions by Eq. 8 Are shown in Fig. 2 C) (dashed lines) with timescales (τ_i) determined from the rotational diffusion constants [6] in Table I. The prefactors A_j are given by a fit against overall rotational correlation functions from MD simulations. These parameters were also used to determine new total correlation functions from Eq. 10 together with internal correlation function from MD simulations. The new total correlation functions are shown also in Fig. 2 A) (dashed lines). The fitted correlation functions are indistinguishable from MD simulation results for short lag times with sufficient statistics, indicating that the anisotropic diffusion model (Eq. 8) and separation of internal and global motions (Eq. 6) are good approximations for the studied system.

The new correlation function can be then used to calculate spectral density from Eqs. 11-12 and spin relaxation times from Eqs. 1-3. The advantage of this approach is that the statistical fluctuations with longer lag times do not interfere the spin relaxation rate calculations. The higher precision is essentially achieved by assuming the anistropic diffusion behaviour, which allows the determination of global rotational correlation functions from diffusion constants. Diffusion constants can be determined by fitting a single parameter to a linear slope which is more robust than fitting exponential function with several parameters to a correlation function calculated from MD simulation. In addition, diffusion constants can be scaled with a constant factor before calculating the new correlation functions to compensate the overestimated rotational diffusion due to inaccuracies in some water models.

The analysis is exemplified for PsTonB and HpTonB-92 proteins in below sections. Spin relaxation rates for all bonds of the proteins are calculated. Global and internal dynamics form MD simulations is compared with NMR data to interpret the experiments and asses simulation model quality.

B. Global rotational dynamics in simulations and experiments

Spin relaxation times calculated from MD simulations for PaTonB and HpTonB-92 with different water models are shown together with experimental data [**?**] in Figs. 3 and 4, respectivelty. The correlation functions as in Eq. 10 were used

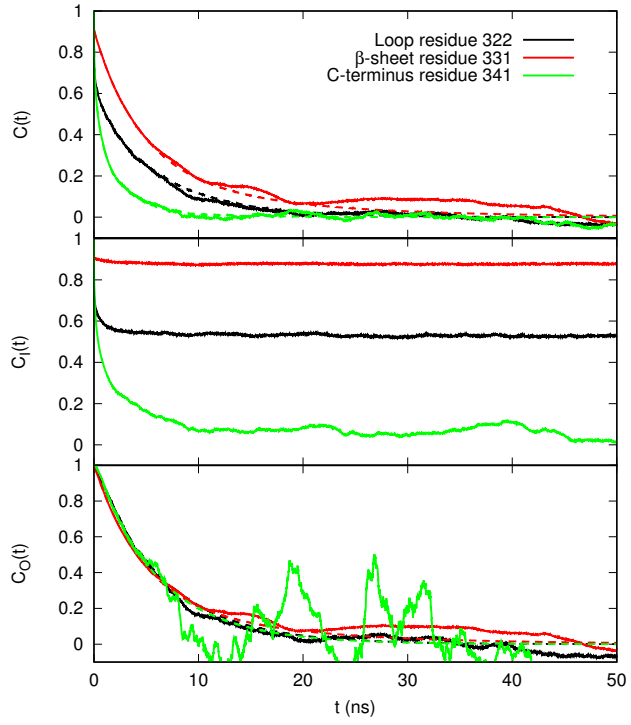

FIG. 2. Rotational correlation functions calculated from MD simulations of PsTonB with tip4p water model at 298K for residues at different regions. A) total correlation functions $C(t)$ calculated from MD simulation (solid lines) and new correlation functions determined from Eqs. 6 and 8 by using rotational diffusion constants and fitted prefactors (dashed lines), B) correlation functions for internal motions calculated from simulation with removed overall protein rotation C) correlation function for overall motions determined as $C_O(t) = C(t)/C_I(t)$ (solid lines) and by fitting to Eq. 8 with timescales from rotational diffusion coefficients in Table I (dashed lines).

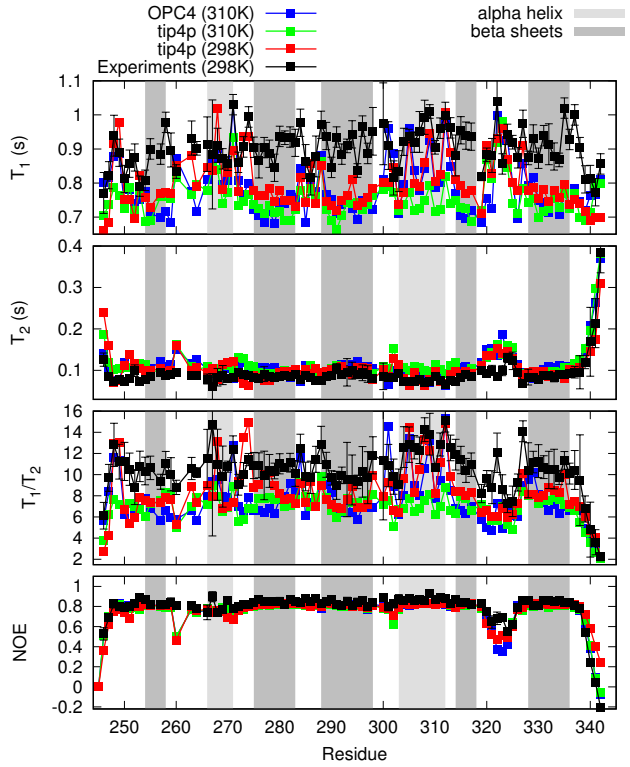

FIG. 3. A) Structures sampled by PsTonB from MD simulations (100 structures from 400ns long trajectory). Alpha helixces are shown with red, beta sheets with blue and residues 246-251, 320-326 and 338-342 with increased internal dynamics are colored yellow. Alphahelix sampling between two orientations (residues 266-270) is shown with pink in left column. B) Spin relaxation rates, order parameters and effective internal correlation times from experiments and simulations.

in the calculations with overall rotational timescales from diffusion constants, prefactors from the fit to the MD simulation data and internal correlation functions from MD simulations. The spectral densities were determined with Eqs. 11-12 and spin relaxation times were then calculated with Eqs. 1-3.

All PsTonB simulations systemically underestimate T_1 values, while T_2 values are in good agreement with experiments. HpTonB-92 simulation with tip4p water gives a relatively good agreement with experiments for all relaxation rates, but simulation with tip3p water model is significantly off from experiments. Importantly, the T_1/T_2 ratios are underestimated in PsTonB simulations and HpTonB-92 simulation with tip3p water model, suggesting that the global rotational diffusion is overestimated in these simulations [**?**]. The overestimation of rotational dynamics simulations with tip3p has been noted also previously [22] and it is typically overcame by introducing isotropic rotational diffusion term in the correlation functions [**?**] or correcting overall rotation by using quaternions [**?**]. Here we scale the diffusion coefficients with a constant factor before calculing the new correlation functions from Eq. 10 to compensate the overestimated overall rotational dynamics.

Spin relaxation times calculated from correlation functions with scaled rotational diffusion constants are shown in Figs. 5 and 6 for PsTonB and HpTonB, respectively. The scaling factors were adjusted to bring T_1/T_2 ratio in optimal agreement with experiments, which resulted scaling factor of 1.2 for PsTonB simulation with tip4p and factor 2.9 for HpTonB with tip3p. Good agreement with experiments suggests that the correlation functions with the scaled diffusion coefficients can be used to interpret the protein rotational dynamics from NMR relaxation data. The scaled rotational diffusion coefficients in Table II are in line with values previously determined for more isotropic proteins [**?**]. The scaled diffusion coefficients for HpTonB-92 with tip3p water model is slightly smaller than with tip4p water model in Table I, which also gave a relatively good agreement with experiments for spin relaxation times. However, a careful comparison reveals that the scaled results with tip3p water model are generally closer to experiments and are thus considered a better interpretation of experiments.

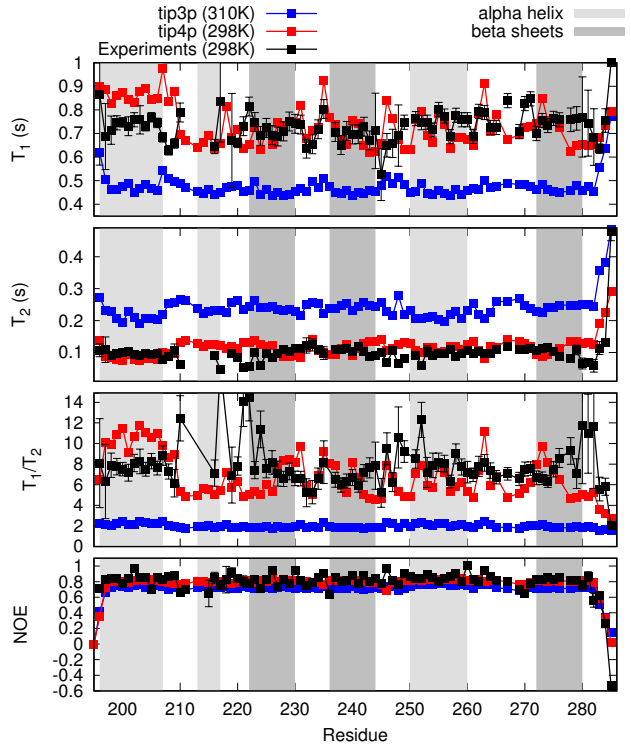

FIG. 4. Relaxation parameters for HpTonB short construct from experiments and simulations with Amber-ildn and different water models

TABLE II. Rotational diffusion coefficients scaled with constant factor which gives a good agreement for spin relaxation data, 2.9 for tip3p simulation of HpTonB and by 1.2 for tip4p simulation of PsTonB.

	HpTonB-92	PsTonB
D_{xx}	2.15 ± 0.01	1.51 ± 0.01
D_{yy}	2.43 ± 0.01	1.72 ± 0.03
D_{zz}	4.10 ± 0.01	3.79 ± 0.03
D_{av}	2.90 ± 0.03	2.3 ± 0.02
τ_c(ns)	5.7 ± 0.1	7.2 ± 0.1

C. Interpretation of protein internal relaxation from MD simulations

Spin relaxation rates from tip4p simulations for PsTonB are in good agreement with experimetns (see Figs **??**), thus the simulations can be used to give interpretation for rotational relaxation processes in proteins, which correspond the NMR relaxation results. Spin relaxation rate deviations from baseline are observed for residues 246-251 in N-terminus, residues 320-326 and residues 338-342 in C-terminus. These segments are coloured in yellow in Fig. **??** A), which already revels ecnhanged conformational sampling in these regions. Also order parameters are low and effective internal relaxation times long for these segements as seen in Fig. **??** B).

More detailed interpretation of different relaxation processes experienced by different residues can be done by analysing timescales which leads in simulation model to the spin relaxation rates in agreement with experiments. Prefactors from Eq. **??** fitted in rotational correlation functions in agreement with spin relaxation data are shown in Fig 7 for

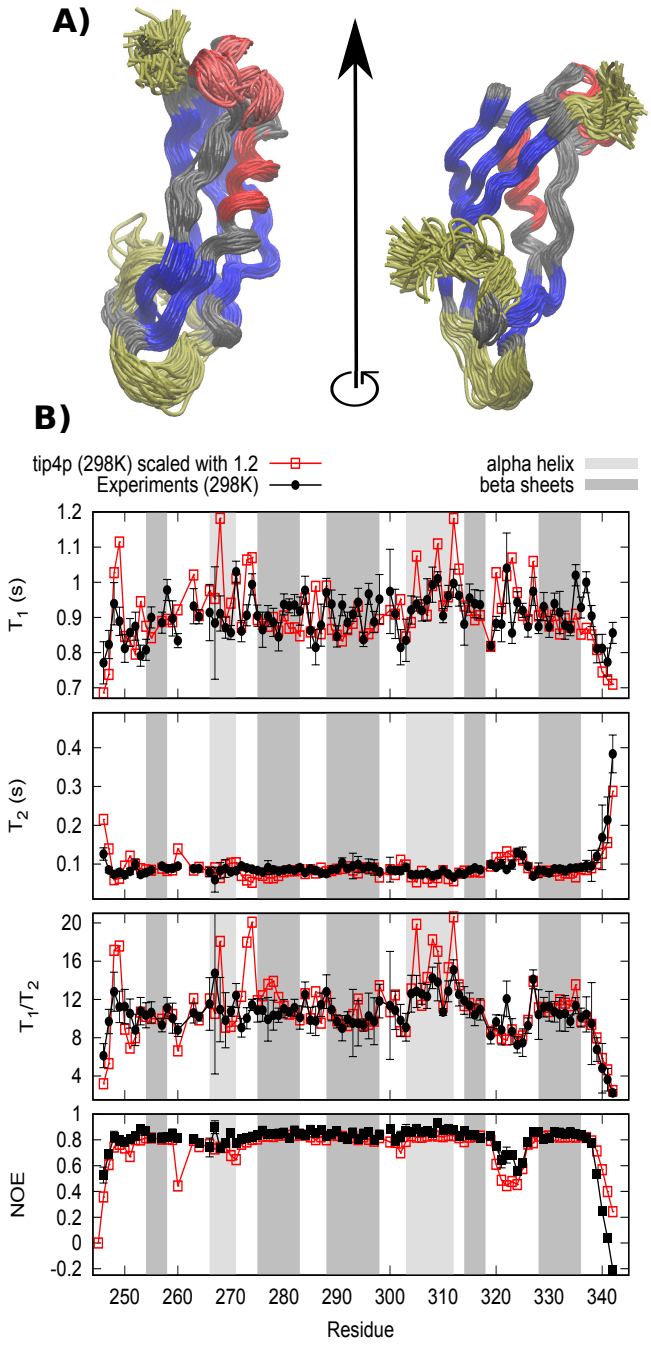

FIG. 5. Relaxation parameters for PsTonB from experiments and simulations with Amber-ildn and different water models. Overall rotational diffusion corrected with factor 1.2. In any publication of scientific results based in part or Info) completely on the use of the program STRIDE, please reference: Info) Frishman,D and Argos,P. (1995) Knowledge-based secondary structure Info) assignment. Proteins: structure, function and genetics, 23, 566-579.

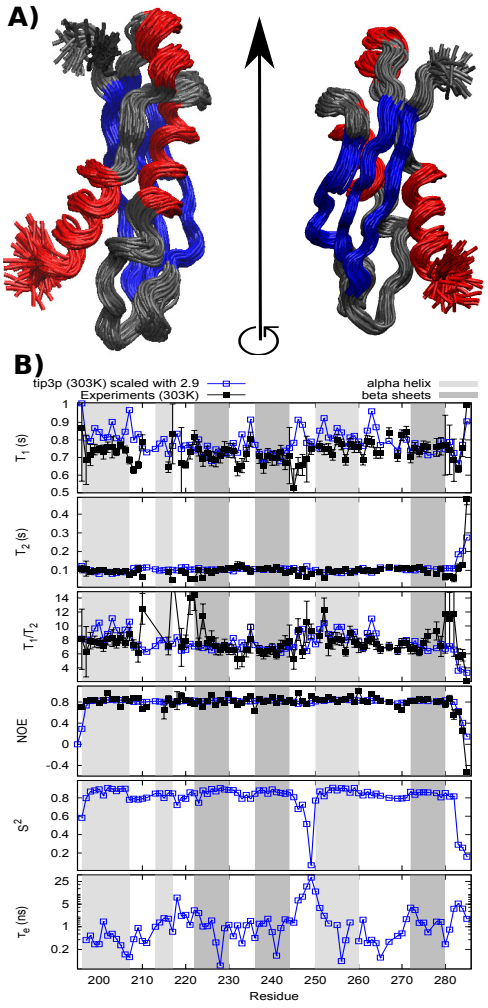

FIG. 6. Relaxation parameters for HpTonB short construct from experiments and simulations with Amber-ildn and different water models

different residues in PsTonB. Residue 331 represents the last alpha helix before C terminus and its rotational relaxation is mostly dominated by relaxations with timescales ∼5.5 ns and ∼8 ns, which arise from global rotation of protein an only small fraction of relaxation arises from fast internal motions, in accordance with large order parameter value (??). Relaxation of residue 322 is also dominated by relaxation processes with timescale around ∼8 ns, but fast motions related to internal protein dynamics are more significant than for alpha helix residue 331. This explains the low order parameter (??) measured small NOE and large T_2 relaxation times values shown in Fig. **??**. Rotational dynamics of residue 341 located in N terminus is dominated by the fast motions related to the internal protein relaxation, as expected from the low order parameter. The contribution from timescales close to ∼13 ns are probably related to slower conformational sampling of the N terminus, which is also seen in sampled conformations and large effective correlation times in Fig. **??**.

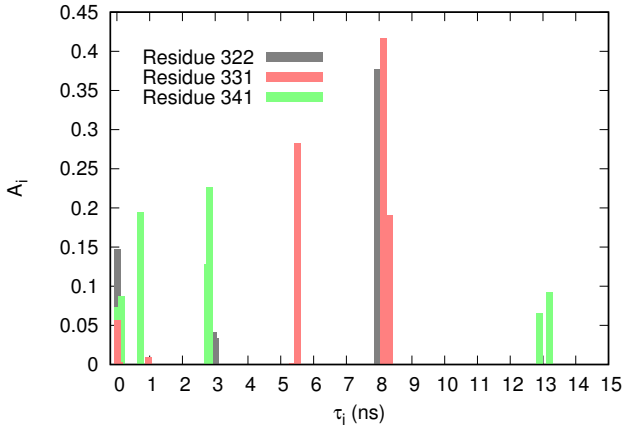

FIG. 7. Prefactors A_i corresponding different timescales τ_i in Eq.**??** resulting from a fit in correlation functions giving good agreement with spin relaxation rates in experimetns for PsTonB.

In addition, low order parameters and larger effective correlation times are observed for PsTonB residues 260-274 and 300-303 in Fig. 3 B). For residues 260-274 this can be explained by two different orientations sampled by alpha helix on that region, as highlighted with pink in Fig. 3 A). This explains also the lower resolution in NMR spectra observed for this and similar region in HpTonB structures [**?**]. Low order parameters and large effective correlation times between residues 300-303 are not seen in spin relaxation data, thus it is not clear if these arise from simulation artefact.

Spin relaxation rate deviations from baseline are observed only few residues in terminal ends for HpTonB-92 as seen in Fig. **??**. This is the case also in simulations, except that the N terminus flexibility seems to be somewhat overestimated and low order parameters and long effetive correlation times are also observed for residues 245-250. The latter observation probably arises (at least partly) from simulation artefacts because deviation form experimental relaxation data is relatively large for these residues. More detailed discussion together with longer HpTonB construct is presented elsewhere [**?**].

IV. CONCLUSIONS

Rotation of protein intertia axes is observed to experience linear diffusion behaviour and overall diffusion component of rotational correlation functions of individual N-H bonds can can be successfully fitted to the model assuming anitropic diffusion for whole molecule.

Rotational diffusion of whole molecules is overestimated by a factor of ∼3 in simulations with tip3p water, in agreement with previous studies [**?**]. The simulations with tip4p and opc4 water models give more realistic diffusion coefficients, which overestimate diffusion only with factors ∼1-1.2.

The overstimated overall diffusion coefficient can be corrected post-simulationally to compare internal dynamics and order with experiments.

The presented methodology can be used to interpret spin relaxation experiments by using MD simulations [**?**] and asses the quality of protein force fields against NMR experiments.

The presented scaling of overall anisotropic diffusion allows this also for simulations with incorrect rotational diffusion due to water models, which is the case in simulations with tip3p.

ACKNOWLEDGMENTS

[1] V. A. Jarymowycz and M. J. Stone, Chemical Reviews **106**, 1624 (2006).

[2] D. Korzhnev, M. Billeter, A. Arseniev, and V. Orekhov, Progress in Nuclear Magnetic Resonance Spectroscopy **38**, 197 (2001).

[3] .

[4] A. Abragam, *The Principles of Nuclear Magnetism* (Oxford University Press, 1961).

[5] L. E. Kay, D. A. Torchia, and A. Bax, Biochemistry **28**, 8972 (1989).

[6] $\tau_1 = (4D_{xx} + D_{yy} + D_{zz})^{-1}$, $\tau_2 = (D_{xx} + 4D_{yy} + D_{zz})^{-1}$, $\tau_3 = (D_{xx} + D_{yy} + 4D_{zz})^{-1}$, $\tau_4 = [6(D + (D^2 - L^2)^{-1/2}]^{-1}$, $\tau_5 = [6(D - (D^2 - L^2)^{-1/2}]^{-1}$, $D = \frac{1}{3}(D_{xx} + D_{yy} + D_{zz})$ and $L^2 = \frac{1}{3}(D_{xx}D_{yy} + D_{xx}D_{zz} + D_{yy}D_{zz})$.

[7] M. J. Abraham, T. Murtola, R. Schulz, S. Pll, J. C. Smith, B. Hess, and E. Lindahl, SoftwareX **12**, 19 (2015).

[8] K. Lindorff-Larsen, S. Piana, K. Palmo, P. Maragakis, J. L. Klepeis, R. O. Dror, and D. E. Shaw, Proteins: Structure, Function, and Bioinformatics **78**, 1950 (2010).

[9] W. L. Jorgensen, J. Chandrasekhar, J. D. Madura, R. W. Impey, and M. L. Klein, J. Chem. Phys. **79**, 926 (1983).

[10] S. Izadi, R. Anandakrishnan, and A. V. Onufriev, The Journal of Physical Chemistry Letters **5**, 3863 (2014).

[11] A. Ciragan, A. S. Aranko, I. Tascon, and H. Iwa, Journal of Molecular Biology **428**, 4573 (2016).

[12] G. Bussi, D. Donadio, and M. Parrinello, J. Chem. Phys. **126** (2007).

[13] M. Parrinello and A. Rahman, J. Appl. Phys. **52**, 7182 (1981).

[14] T. Darden, D. York, and L. Pedersen, J. Chem. Phys. **98**, 10089 (1993).

[15] U. L. Essman, M. L. Perera, M. L. Berkowitz, T. Larden, H. Lee, and L. G. Pedersen, J. Chem. Phys. **103**, 8577 (1995).

[16] B. Hess, J. Chem. Theory Comput. **4**, 116 (2008).

[17] M. Abraham, D. van der Spoel, E. Lindahl, B. Hess, and the GROMACS development team, *GROMACS user manual version 5.0.7* (2015).

[18] R. T. McGibbon, K. A. Beauchamp, M. P. Harrigan, C. Klein, J. M. Swails, C. X. Hernández, C. R. Schwantes, L.-P. Wang, T. J. Lane, and V. S. Pande, Biophysical Journal **109**, 1528 (2015).

[19] .

[20] A. Nowacka, N. Bongartz, O. Ollila, T. Nylander, and D. Topgaard, J. Magn. Res. **230**, 165 (2013).

[21] T. M. Ferreira, O. H. S. Ollila, R. Pigliapochi, A. P. Dabkowska, and D. Topgaard, J. Chem. Phys. **142**, 044905 (2015).

[22] V. Wong and D. A. Case, The Journal of Physical Chemistry B **112**, 6013 (2008).

SUPPLEMENTARY INFORMATION

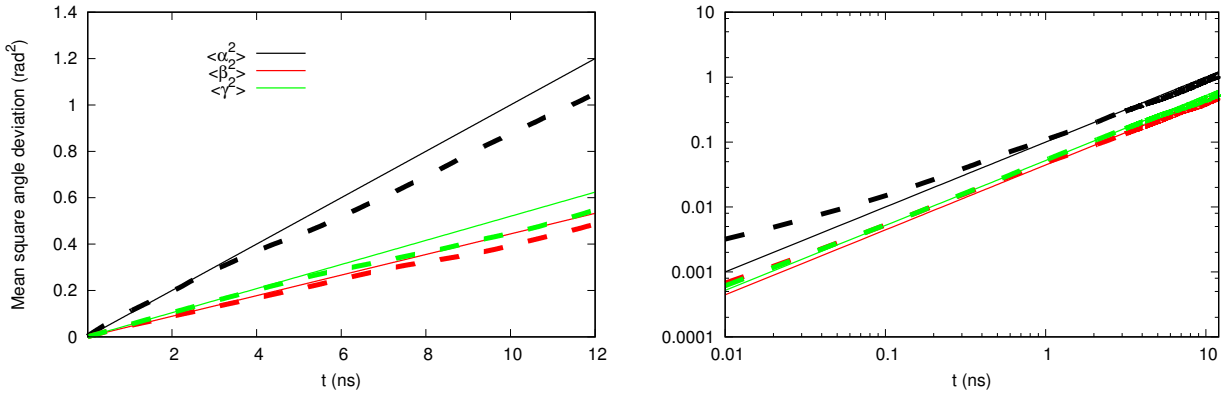

FIG. 8. The intertia tensor angles as a function of time and mean square angular deviations for PsTonB simulation with OPC water model.

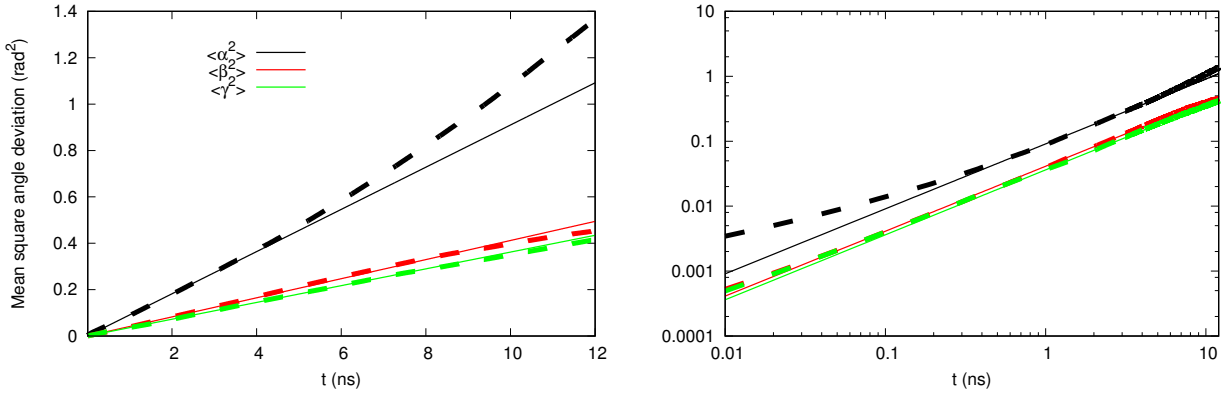

FIG. 9. The intertia tensor angles as a function of time and mean square angular deviations for PsTonB simulation with OPC water model.